Geometry-Controlled Interface Localization-Delocalization Transition in Block Copolymers

Marcus Müller*

Institut für Theoretische Physik, Georg-August-Universität, 37077 Göttingen, Germany

(Received 26 April 2012; published 24 August 2012)

Lamellar copolymers confined into a film of thickness D by two stripe-patterned surfaces, which are rotated against each other by a twist angle α, form lamellar domains that register and align with the respective chemical surface patterns. The two domains of thickness x and $D - x$ are separated by an interface that resembles a twist grain boundary. At small twist angles α or strong selectivity of the surface patterns, this interface fluctuates around the middle of the film, $x \approx D/2$, while the interface is localized at one of the surfaces, $x \approx 0$ or $x \approx D$, in the opposite limit. These two morphologies are separated by an interface localization-delocalization transition (ILDT) that can be controlled by the twist angle α. For thin films, we find a second-order ILDT while the ILDT is first-order for large D values. A phenomenological interface Hamiltonian is used to relate the findings to the ILDT of symmetric mixtures, and the predictions are confirmed by molecular simulation.

DOI: 10.1103/PhysRevLett.109.087801 PACS numbers: 61.20.Ja, 64.75.Jk, 64.75.Yz, 82.35.Jk

Block copolymers are amphiphilic molecules that self-assemble into spatially periodic structures. The length scale of this microphase is dictated by the interplay between the free-energy cost of the internal AB interfaces, favoring a large periodicity, λ_0, and the concomitant loss of configurational entropy. λ_0 is comparable to the molecules' end-to-end distance, R_{e0}, i.e., in the range of 10–100 nm. In the following, we consider symmetric AB diblock copolymers that self-assemble into a lamellar phase in the bulk [1,2].

Confining such a spatially modulated phase into a thin film, geometrical constraints, or interactions with the confining surfaces can induce phase transitions [3–8]. The transition between lamellar phases with parallel and perpendicular orientations induced by the mismatch between the film thickness and the bulk periodicity has attracted abiding interest. Strong confinement can also induce new morphologies, e.g., the hexagonally perforated phase.

Utilizing a chemically patterned bottom substrate and a nonpreferential top surface, one can direct the assembly of copolymer materials. If the two-dimensional chemical surface pattern coincides in symmetry and length scale with the bulk morphology, the chemical pattern will be replicated without defects [9,10]. Deviations between the surface pattern and the bulk morphology, however, may lead to novel structures [11]. (i) If the periodicity of the stripe pattern, λ_b, is much larger than the lamellar spacing, λ_0, in the bulk, the copolymer will replicate the surface pattern in a thin layer at the chemically patterned surface (surface reconstruction) but will adopt a lamellar morphology with periodicity, λ_0, away from the surface [12]. The interface between the registered substrate morphology and the bulk morphology on top resembles a grain boundary. (ii) If the surface pattern differs in geometry from the bulk morphology, the surface reconstruction may lead to complex bicontinuous morphologies with no analogue in the bulk phase diagram [13].

Recently, the morphology of copolymer films confined between two surfaces with orthogonal stripe patterns has been studied by experiment and simulation [14,15]. The copolymer replicates the stripe pattern at the respective surface, and the orthogonally oriented lamellar domains meet around the center of the film forming an interface (twist grain boundary) that resembles Scherk's first minimal surface.

In this Letter, we show that this system exhibits an interface localization-delocalization transition (ILDT) and discuss the relation to the ILDT in symmetric binary mixtures [16–23]. The ILDT is the analogue of a wetting transition in a thin film with antisymmetric boundary conditions. Consider two phases (e.g., an A-rich and a B-rich phase of a binary AB mixture or two lamellar phases with different orientations) that coexist in the bulk. If one brings the system in contact with a surface that is only weakly preferential, the preferred phase will form a microscopically thin layer at the surface (nonwet). Upon increasing the surface preference, one encounters a wetting transition, where the thickness of the preferred phase diverges; i.e., the preferred phase wets the surface [22,24,25]. In an antisymmetric film, where the bottom surface prefers one of the coexisting bulk phases with exactly the same but opposite strength than the top surface prefers the other coexisting phase, domains of the coexisting phases form at the respective surfaces. If the surface preference is strong, the interface that separates these two domains will run parallel to the film surfaces and will fluctuate around the middle of the film in this delocalized state. If the surface preference is small, in turn, the interface will be localized at one of the surfaces. The transition between these two states, which is illustrated in Fig. 1, is the ILDT,

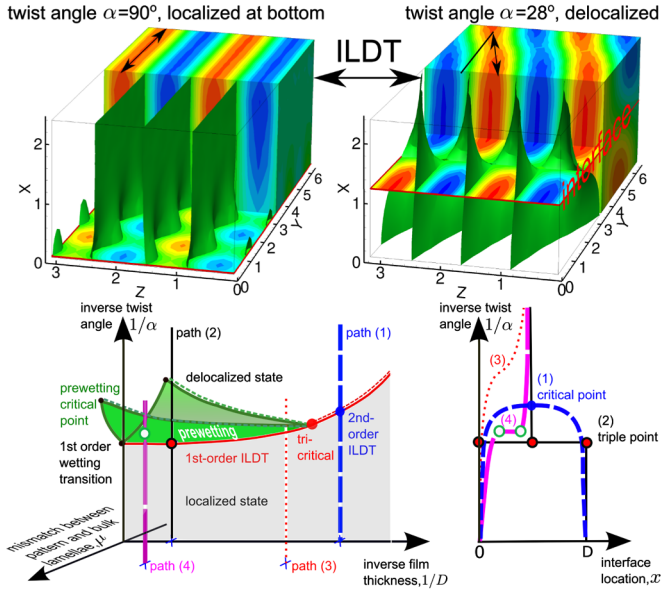

FIG. 1 (color online). (top) Contour plots of the time-averaged composition of the localized and delocalized state for $\Lambda N = 0.035$ and twist angles $\alpha = 90°$ ($m < 0$) and 28°, respectively. The position of the interface, $x \approx 0$ (localized) and $x = D/2$ (delocalized), is indicated by a plane. The green surfaces show the internal AB interfaces of the microphase. (bottom, left) Sketch of the ILDT as a function of inverse film thickness, inverse twist angle, and mismatch between the pattern and bulk lamellae, $\mu \sim B[(\lambda_b - \lambda_0)^2 - (\lambda_t - \lambda_0)^2]$. Paths (1) and (2) in the plane $\mu = 0$ correspond to a second- and first-order ILDT, respectively; $\mu > 0$ for paths (3) and (4). Path (3) does not show any singularity of the interface position, while path (4) crosses the surface of prewetting transitions. (bottom, right) Position x of the interface as a function of $1/\alpha$ for the four paths.

and it occurs close to the wetting transition of the semi-infinite system [16].

While the ILDT has attracted much interest in theory and simulation [16–18,20–23], it is difficult to observe experimentally. Generically, neither are the coexisting bulk phases strictly symmetric nor are the surface interactions strictly antisymmetric. In the absence of these stringent symmetry requirements, however, one observes a gradual crossover between ILDT and capillary condensation, which occurs for symmetric boundary conditions [26]. Copolymers confined between two chemically patterned surfaces is a unique system that fulfills the stringent symmetry requirements for ILDT: Since the two microphases only differ by their orientation, they are strictly symmetric [27]. Using the same chemically patterned surfaces, which are twisted by an angle α, one also fulfills the requirement of strictly antisymmetric surface interactions without fine-tuning of the microscopic interactions.

We discuss the qualitative behavior by describing the complex morphology (cf., Fig. 1) only by the position, x, of the interface between the two lamellar domains (grains) in the film of thickness D. The free energy of the system takes the schematic form

$$\frac{\Delta F(x)}{A} = \gamma_b(\Lambda) + \gamma_t(\Lambda) + \gamma(\alpha) + \frac{1}{2}B(\lambda_b - \lambda_0)^2 x + \frac{1}{2}B(\lambda_t - \lambda_0)^2(D - x) + g_b(x) + g_t(D - x). \quad (1)$$

γ_t and γ_b are the surface tensions of the block copolymer morphology replicating the top and bottom surface patterns, respectively. Λ characterizes the strength of the surface interactions. $\gamma(\alpha)$ denotes the free energy per area of the interface that depends on the twist angle, α, between the two lamellar grains. The second line accounts for the free-energy increase of the domains due to a mismatch between the bulk periodicity, λ_0, and the periods, λ_b and λ_t, of the bottom and top surface patterns. B is the bulk compression modulus of the lamellar phase. The third line describes the effective interaction per area between the interface (twist grain boundary) and the patterned surfaces, $g_b(x)$ and $g_t(x)$. These interface potentials are short-ranged, and their characteristic length, ξ, is set by the spatial extent of the distortion of the lamellar structure due to the surfaces or the interface, $\xi \sim \lambda_0 \sim R_{e0}$. They vanish for $x \to \infty$. In the opposite limit, $g_b(x_{min}) = \Delta\gamma_b - \gamma$, where $x_{min} \approx 0$ for a strong first-order wetting transition. $\Delta\gamma_b > 0$ is the difference in surface free energies at the bottom between the lamellar domain that is aligned with the top surface and the lamellar structure that is aligned with the bottom surface. The minimal form of the interface potential in the vicinity of a first-order wetting transition is $g_b(x) + g_t(D - x) \propto \tilde{m}^2(\tilde{m}^2 - r)^2 + t\tilde{m}^2$ with $\tilde{m}^2 = 2\exp(-D/2\xi)\{\cosh([x - D/2]/\xi) - 1\}$, where r and t are constants that depend on the surface interactions [21,28]. This interface Hamiltonian gives rise to a rich behavior, which is qualitatively illustrated in Fig. 1.

Equation (1) implies that the ILDT can be controlled by geometrical parameters of the system: In the semi-infinite system, the aligned registered lamellar domain will wet the chemically patterned surface if the difference $\Delta\gamma_b$ exceeds the interfacial free energy, $\gamma(\alpha)$. In the simplest approximation, $\Delta\gamma_b$ can be estimated by the interaction energy with the surface, which is approximately independent from α. The interfacial free energy, γ, in turn, decreases with α and vanishes for $\alpha \to 0$ [29]. Thus, we expect that the interface will be delocalized around the center of the film for any finite strength of the surface interaction in the limit of vanishing α.

If the wetting transition is first-order, the ILDT in a thick film will also be first-order (path 2 in Fig. 1). There is a line of triple points, where the delocalized state and the two localized states have the same free energy. Upon reducing the film thickness, the order of the ILDT changes from first to second (critical, path 1) at a tricritical film thickness, D_{tc}. For $D < D_{tc}$, the two localized states continuously merge into the delocalized state.

Another difference between the IDLT of binary mixtures and the geometry-controlled ILDT in spatially modulated

phases of copolymers is the absence of the conservation of the order parameter. Thus there is no analogue of a miscibility gap, and generically one controls the thermodynamical variable conjugated to the order parameter. In a symmetric binary AB mixture, the order parameter is the amount of A, and the conjugated variable is the chemical potential. In case of the geometry-controlled ILDT of spatially modulated phases, the mismatch between the periodicity of the surface pattern and the bulk morphology plays the role of the chemical potential, $\mu \sim B[(\lambda_b - \lambda_0)^2 - (\lambda_t - \lambda_0)^2]$.

We use molecular simulations of a minimal, soft, coarse-grained model to examine the predictions of this schematic model. The n symmetric AB block copolymers are represented by chains of $N = 16$ beads. The Hamiltonian $\mathcal{H}$ is comprised of bonded, nonbonded, and surface interactions [30,31]. The bonded interactions take the form of a bead-spring model, $\frac{\mathcal{H}_b}{k_B T} = \sum_{t=1}^{N-1} \frac{3(N-1)}{2R_{e0}^2}[\mathbf{r}_{i,t+1} - \mathbf{r}_{i,t}]^2$, where R_{e0} is the end-to-end distance of the noninteracting copolymers, and $\mathbf{r}_{i,t}$ denote the coordinate of the tth bead on molecule, i. The nonbonded interactions are given by

$$\frac{\mathcal{H}_{nb}}{k_B T\sqrt{\bar{\mathcal{N}}}} = \int \frac{d\mathbf{r}}{R_{e0}^3}\left[\frac{\kappa_0 N}{2}(\hat{\phi}_A + \hat{\phi}_B - 1)^2 - \frac{\chi_0 N}{4}(\hat{\phi}_A - \hat{\phi}_B)^2\right]$$

with $\hat{\phi}_A(\mathbf{r}) = \frac{1}{\rho_0}\sum_{i,t}\Theta_A(i,t)\delta(\mathbf{r} - \mathbf{r}_{i,t})$. Here, $\Theta_A(i,t) = 1$ if the bead t on molecule i is of type A and zero otherwise. $\kappa_0 N = 50$ limits fluctuations of the total density from the reference value, $\rho_0 = nN/V$. $V = D \times L_y \times L_z$ is the volume. $\chi_0 N = 20$ describes the repulsion between A and B beads. $\bar{\mathcal{N}} = (\rho_0 R_{e0}^3/N)^2 = 64^2$ characterizes the molecular density. The interaction with the surface takes the form [11]

$$\frac{\mathcal{H}_s}{k_B T\sqrt{\bar{\mathcal{N}}}} = -\frac{\Lambda N R_{e0}}{\epsilon}\int \frac{d\mathbf{r}}{R_{e0}^3}(\hat{\phi}_A - \hat{\phi}_B)(f_b(y,z)e^{-x^2/2\epsilon^2} + f_t(y,z)e^{-(D-x)^2/2\epsilon^2}),$$

where the functions f_b and f_t describe the surface patterns as a function of the lateral coordinates, y, z. They adopt the values ± 1 on the respective stripes. We discretize space in cells of linear dimensions, $\Delta L \approx R_{e0}/6$ in order to express the local densities, $\hat{\phi}_A$ and $\hat{\phi}_B$, explicitly in terms of the bead coordinates. Smart Monte Carlo (MC) moves have been used to update the molecular conformations and, in some runs, we additionally attempted to swap the A and B blocks of a copolymer. At $\chi_0 N = 0$, the relaxation time is $\tau = R_{e0}^2/D_{cm} = 2833$ MC steps, where D_{cm} is the self-diffusion coefficient. Simulation runs extend up to 2×10^7 MC steps.

In contrast to experiment, the periodic boundary conditions in y and z directions in conjunction with the collocation used to compute $\hat{\phi}_A$ and $\hat{\phi}_B$ make it difficult to continuously vary the twist angle α and, therefore, we additionally study the dependence on ΛN. Since the two blocks are structurally symmetric and the surface interactions are symmetric, the surface free energy is dominated by the surface energy [32]. The surface energy of a misaligned lamellar domain approximately vanishes. The surface energy of a perfectly aligned and registered morphology in the strong segregation limit is $-\sqrt{\pi/2}\Lambda N\sqrt{\bar{\mathcal{N}}}k_B T/R_{e0}^2 = -\Delta\gamma_b$. The interface tension $\gamma(\alpha = 90°)$ also is of the order $0.1\sqrt{\bar{\mathcal{N}}}k_B T/R_{e0}^2$ [29]. Thus, the ILDT is expected to occur for $\Lambda N \leq 0.1$.

Rather than explicitly locating the interface, we employ the order parameter $m \equiv \frac{1}{V}\int d\mathbf{r}(f_b - f_t)(\hat{\phi}_A - \hat{\phi}_B)$. At strong segregation, ideally, $m = 1$ if the domain, which is aligned with the bottom surface, pervades the entire film and the interface is localized at the top of the film. At $m = 0$, the interface is located at the center, $x = D/2$, of the film, and $m = -1$ if the entire morphology aligns with the top surface pattern, and $x \approx 0$. At $\chi_0 N = 20$ and $\bar{\mathcal{N}} = 64^2$ (cf., snapshots in Fig. 1), however, the lamellar morphology exhibits composition fluctuations and the width of the internal AB interfaces is finite. Additionally, if the interface is localized at $x \approx 0$, there is some distortion of the morphology in the ultimate vicinity of the bottom surface. Therefore, the order parameter does not adopt its limiting values.

In Fig. 2 we present the order-parameter distribution for $D = 1.234R_{e0}$ and $\alpha = 90°$ for various values of ΛN. For small strength of the surface interactions, the

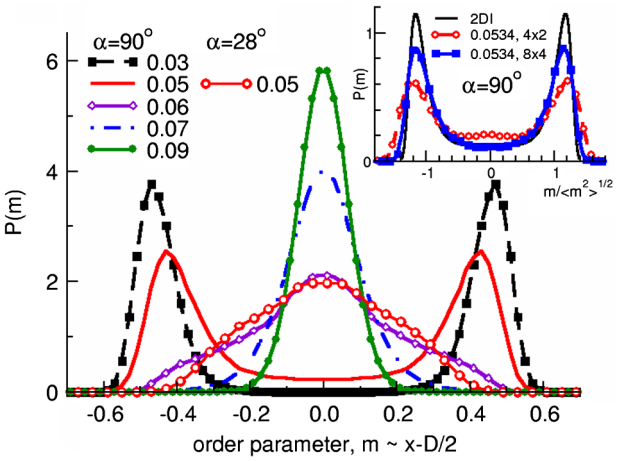

FIG. 2 (color online). Probability distribution, $P(m)$, of the order parameter for a thin film, $D = 1.234R_{e0}$, $L_y = 2L_z = 6.38R_{e0} \approx 4\lambda_0$. The apposing surface patterns are orthogonal, $\alpha = 90°$, and the strength of the surface interaction, ΛN, is indicated in the key. Data for $\alpha = 28°$ and $\Lambda N = 0.05$ are also included. The inset compares $P(m)$, scaled to unit variance, at ΛN_c for two different lateral system sizes, $4\lambda_0 \times 2\lambda_0$ and $8\lambda_0 \times 4\lambda_0$, with the order-parameter distribution of the 2D Ising model with aspect ratio 1:2.

distribution is double-peaked, indicating that the interface is localized at one of the apposing surfaces. At large ΛN, the distribution is centered around $m = 0$ and the interfaces is delocalized at the film center. The bimodal distribution of the localized state gradually transforms into a single peak centered around $m = 0$. Thus, for this thin film, the ILDT at $\Lambda N_{\mathrm{crit}} \approx 0.0534(10)$ is second-order. The inset depicts the distribution of the order parameter normalized to unit variance for two different lateral system sizes and compares the distribution to that of the two-dimensional Ising model with the same aspect ratio. Given the very limited lateral system size, we judge this agreement to corroborate the anticipated 2D Ising critical behavior of the ILDT.

The main panel of Fig. 2 also includes the result for $\alpha = 2\arctan(1/4) \approx 28°$, $L_y = 2L_z = 4\lambda_0/\cos(\alpha/2)$ and $\Lambda N = 0.05$. For this smaller twist angle, the interface tension is low and the interface is delocalized in the middle of the film, whereas for $\alpha = 90°$ the interface is predominantly localized at a surface.

Figure 3 shows the distribution function for a greater film thickness. For small ΛN, the distribution also is bimodal, indicating that the interface is localized at one of the two apposing surfaces. For intermediate values, however, it exhibits a trimodal form, and for large ΛN values the middle peak dominates, characteristic for the delocalized state. This behavior indicates that the ILDT is first-order in the thicker film. The triple point can be estimated by the equal-area rule, yielding $\Lambda N_{\mathrm{tri}} \approx 0.0396(10)$. A crossover from a critical to a first-order ILDT upon increase of D has previously been predicted

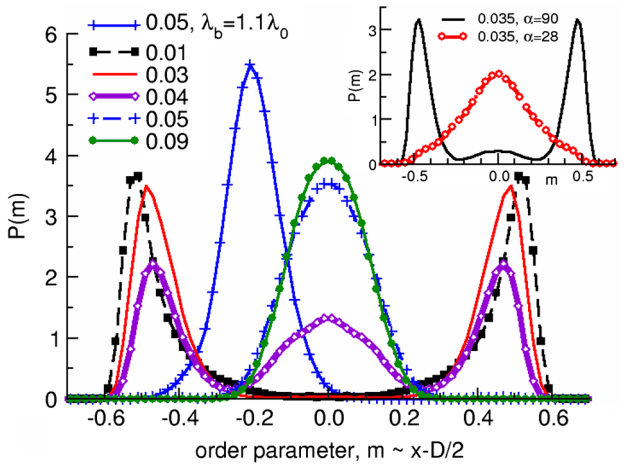

FIG. 3 (color online). Probability distribution, $P(m)$, of the order parameter for a thick film, $D = 2.468R_{e0}$, $L_y = 2L_z = 2\lambda_0$, and various values of ΛN. The pattern periodicities of the orthogonal bottom and top patterns are identical, $\lambda_b = \lambda_t = \lambda_0$, except for the first data set, where $\lambda_b = 1.1\lambda_0$ results in an asymmetric distribution. The inset compares the distribution of orthogonal patterns, $\alpha = 90°$, with $P(m)$ of a less twisted system, $\alpha = 28°$.

[20]. The film thickness of the concomitant tricritical transition is of the order of the range, ξ, of interaction between interface and surface.

Additionally, Fig. 3 presents the probability distribution, $P(m)$, between two orthogonal stripes with different pattern periods, $\lambda_t \approx \lambda_0$ and $\lambda_b \approx 1.1\lambda_0$. Since the lamellae at the bottom have a higher free-energy density, $P(m)$ is no longer symmetric but the interface position is preferentially located in the lower half.

The inset of Fig. 3 depicts the probability distribution for $\Lambda N = 0.054$ and two different twist angles, $\alpha = 90°$ and $\alpha = 2\arctan(1/4) = 28°$. For the orthogonal patterns, the interface is localized at one of the two walls, while for the smaller twist angle the interface fluctuates around the center of the film. This observation confirms the qualitative prediction in Fig. 1, which also depicts time-averaged snapshots of the two morphologies.

In summary, we have demonstrated by phenomenological considerations and molecular simulations that the directed assembly of block copolymers between patterned surfaces exhibits an ILDT. We argue that this is an ideal experimental realization of an ILDT because the stringent antisymmetry of the system is obeyed without fine-tuning of interactions [23,26], which would be necessary for observing the ILDT in a binary mixture or liquid–vapor systems. Moreover, the location of the transition and its order can be controlled by purely geometric characteristics, the twist angle of the patterns and film thickness, respectively. The morphology of the film and the location of the interface is accessibly by small angle x-ray scattering experiments [15], and we hope that our predictions will be confirmed experimentally.

Apart from the rich statistical mechanics of the system, the directed assembly of copolymer materials has attracted abiding interest in pattern formation at the nanoscale. The understanding of the wetting transition or the ILDT is important. (i) In thin supported films, defect removal does not proceed via lateral diffusion and annihilation but by shifting the interface between the registered bottom morphology and the misaligned defect at the top towards the top surface (liquid–vapor interface) of the film [33]. Recently, it was argued that defect formation during the ordering will be strongly suppressed if the preference of the patterned bottom surface is sufficiently strong for the registered domain to wet the patterned surface [34]. (ii) The control of the interface between the two grains, which are aligned with the respective surface patterns, is important for directing the three-dimensional assembly of copolymer materials and fabricating complex morphologies. For instance, the position of the interface can be precisely controlled by the mismatch between the bulk lamellae period and the pattern period.

The knowledge of thermodynamic equilibrium morphologies is an indispensable prerequisite for studying the kinetics of structure formation and transformation, which

may be protracted in experiments [15]. The kinetics can play an important role in the localization of the interface. If one chemical pattern starts the nucleation faster than the other, then the grain induced by the first one is going to be larger than the second one and, initially, the interface is going to be located near the second surface [15].

M. M. thanks A. Ramírez-Hernández and J. J. de Pablo for helpful comments. This research was supported in part by the National Science Foundation under Grant No. NSF PHY05-51164 (NSF-KITP-12-095) and the DFG under Grant No. Mu 1674/11. The author acknowledges the hospitality of the Kalvi Institute for Theoretical Physics, UCSB. Simulations were performed at HLRN Hannover and JSC Jülich, Germany.

*mmueller@theorie.physik.uni-goettingen.de

[1] L. Leibler, Macromolecules **13**, 1602 (1980).
[2] T. Ohta and K. Kawasaki, Macromolecules **19**, 2621 (1986).
[3] D. G. Walton, G. J. Kellogg, A. M. Mayes, P. Lambooy, and T. P. Russell, Macromolecules **27**, 6225 (1994).
[4] G. T. Pickett and A. C. Balazs, Macromolecules **30**, 3097 (1997).
[5] M. W. Matsen, J. Chem. Phys. **106**, 7781 (1997).
[6] T. Geisinger, M. Müller, and K. Binder, J. Chem. Phys. **111**, 5241 (1999).
[7] M. J. Fasolka, P. Banerjee, A. M. Mayes, G. Pickett, and A. C. Balazs, Macromolecules **33**, 5702 (2000).
[8] Q. Wang, P. F. Nealey, and J. J. de Pablo, Macromolecules **34**, 3458 (2001).
[9] S. O. Kim, H. H. Solak, M. P. Stoykovich, N. J. Ferrier, J. J. de Pablo, and P. F. Nealey, Nature (London) **424**, 411 (2003).
[10] M. P. Stoykovich, M. Müller, S. O. Kim, H. H. Solak, E. W. Edwards, J. J. de Pablo, and P. F. Nealey, Science **308**, 1442 (2005).
[11] K. C. Daoulas, M. Müller, M. P. Stoykovich, Y. J. Papakonstantopoulos, J. J. de Pablo, P. F. Nealey, S. M. Park, and H. H. Solak, J. Polym. Sci., Part B: Polym. Phys. **44**, 2589 (2006).
[12] M. Müller, K. C. Daoulas, and Y. Norizoe, Phys. Chem. Chem. Phys. **11**, 2087 (2009).
[13] K. C. Daoulas, M. Müller, M. P. Stoykovich, S. M. Park, Y. J. Papakonstantopoulos, J. J. de Pablo, P. F. Nealey, and H. H. Solak, Phys. Rev. Lett. **96**, 036104 (2006).
[14] A. Ramírez-Hernández, G. Liu, P. F. Nealey, and J. J. de Pablo, Macromolecules **45**, 2588 (2012).
[15] G. Liu, A. Ramírez-Hernández, H. Yoshida, K. Nygård, D. K. Satapathy, O. Bunk, J. J. de Pablo, and P. F. Nealey, Phys. Rev. Lett. **108**, 065502 (2012).
[16] A. O. Parry and R. Evans, Phys. Rev. Lett. **64**, 439 (1990).
[17] M. R. Swift, A. L. Owczarek, and J. O. Indekeu, Europhys. Lett. **14**, 475 (1991).
[18] K. Binder, D. P. Landau, and A. M. Ferrenberg, Phys. Rev. Lett. **74**, 298 (1995).
[19] T. Kerle, J. Klein, and K. Binder, Phys. Rev. Lett. **77**, 1318 (1996).
[20] M. Müller, E. V. Albano, and K. Binder, Phys. Rev. E **62**, 5281 (2000).
[21] M. Müller and K. Binder, Phys. Rev. E **63**, 021602 (2001).
[22] K. Binder, D. Landau, and M. Müller, J. Stat. Phys. **110**, 1411 (2003).
[23] A. D. Virgiliis, R. L. C. Vink, J. Horbach, and K. Binder, Europhys. Lett. **77**, 60002 (2007).
[24] S. Dietrich, *Phase Transitions and Critical Phenomena* (Academic Press, New York, 1988).
[25] J. Chavrolin, J. Joanny, and J. Zinn-Justin, *Liquids at Interfaces*, Les Houches 1988, Session XLVIII (Elsevier, Amsterdam, 1990).
[26] M. Müller, K. Binder, and E. V. Albano, Europhys. Lett. **50**, 724 (2000).
[27] By the same token, long-ranged van der Waals interactions do not influence the location of the interface because the two phases are comprised of the same material.
[28] In the delocalized state, this short-ranged interaction imparts a positive curvature on $\Delta F(x)$ around $x = D/2$, which exponentially decreases with D/R_{e0}. Thus, the interface will strongly fluctuate around the center of the film for small A [14,15].
[29] D. Duque, K. Katsov, and M. Schick, J. Chem. Phys. **117**, 10315 (2002).
[30] K. C. Daoulas and M. Müller, J. Chem. Phys. **125**, 184904 (2006).
[31] M. Müller, J. Stat. Phys. **145**, 967 (2011).
[32] M. Müller and K. Binder, Macromolecules **31**, 8323 (1998).
[33] E. W. Edwards, M. P. Stoykovich, M. Müller, H. H. Solak, J. J. de Pablo, and P. F. Nealey, J. Polym. Sci., Part B: Polym. Phys. **43**, 3444 (2005).
[34] U. Nagpal, M. Müller, P. F. Nealey, and J. J. de Pablo, ACS Macro Lett. **1**, 418 (2012).